# NORTH WIND 4KW 'PASSIVE' CONTROL SYSTEM DESIGN

Hugh Currin
Foehn consulting
Box 5123
Klamath Falls, OR 97601

An overview of a mechanical rotor control design is presented. Operation at constant RPM and rapid response are obtained by using blade pitch moments for both sensing control need and blade pitch actuation. The basic concept, static or equilibrium design, and dynamic analysis are briefly presented.

## INTRODUCTION

The control system described here is part of a SWECS design done for North Wind Power Co. under a Rockwell/DOE contract. The machine, as now configured is a 10 meter, down wind, HAWT rated at 6KW @ 8m/s. It is a line interface unit using a direct drive syncronous alternator. The rotor is a two bladed, teetering system with delta three and uses solid laminated wood blades. The system is free yawing on a guyed wooden pole tower.

The rotor control is an all mechanical system which responds to blade aerodynamic loads and RPM. Power and load control is accomplished through blade pitching in the direction of feather with shut down being full feather. Starting comes from an inboard blade twist.

## CONCEPT

The control system concept is to change blade pitch angle in response to blade pitch moment. The blades are then sensors transmitting control information, and also supplying control actuation force, via blade pitch moment. Pitch moment, through placement of the pitch axis, is made sensitive to aerodynamic and centrifugal forces. This control can thus be used with a rotor operating at constant, synchronous, RPM while still providing protection against overspeed conditions.

Figure 1 shows the pitch axis placement at one radial station. Aerodynamic Lift, the predominant blade force, will create a pitching moment through offset Xa. Equilibrium is obtained by applying the control moment Mc. For a given wind speed there is one equilibrium pitch angle θ. For example, assume θ is increased from an equilibrium position, then the airfoil angle of attack will decrease, reducing the coefficient of lift and thus Lift Force. The aerodynamic moment is now less than the control moment which actuates a blade pitch, decreasing θ, until equilibrium is again reached. This aerodynamic restoring force maintains equilibrium.

For constant RPM operation a change in wind speed will move the system to a new equilibrium pitch angle. The predominant effect of an increase in wind speed is an increase in angle of attack which increases the lift coefficient and Lift force. This difference between aerodynamic and control moments will tend to increase the pitch angle until a new equilibrium point is reached.

The control moment Mc is a function of pitch angle and will determine the equilibrium pitch angle at each wind speed. The rotor power output, being dependant on wind speed and pitch angle, is determined by this Mc function.

Figure 1 also shows the blade center of gravity offset from the rotor axis. This gives a positive (+θ) pitching moment due to rotor angular velocity which results in sensitivity to rotor overspeed.

## STATIC DESIGN

Static Design of this control system involves a trade-off between rotor geometry, control moment characteristics, desired power curve, and resulting unloaded equilibrium overspeed. Figure 2 represents the final geometric layout of the rotor.

To evaluate this analytically a Blade Element Theory for aerodynamic forces (ref 1) is combined with a simple rigid body model for rotational effects. A plot for constant rotor RPM is given in Figure 3. Here the pitch moment, or equilibrium control moment, is given as a function of pitch angle for constant wind speeds and rotor power outputs. Figure 4 presents the same type of plot for zero power output, representing the unloaded control response.

Equilibrium performance is determined by these plots. With control moment given as a function of pitch angle the resulting power, unloaded RPM, and blade pitch are defined as functions of wind speed. Assumed control moment curves are presented in Figures 3 and 4 as dotted lines.

Trade-offs to obtain desireable static performance characteristics involve adjusting rotor geometry, control moment function, and associated structure. Since these involve constraints such as manufacturability and conceptual design they don't lead to explicit evaluation.

## AEROELASTIC

The torsional stiffness of this blade-hub system is inherently very low being predominantly from the aerodynamic restoring force mentioned earlier. Because of this the rotor is susceptable to aeroelastic instabilities.

Modes which involve in-plane motions shouldn't be excited due to the high natural frequencies in this degree of freedom. Following this reasoning, problems of ground resonance and whirl modes aren't anticipated. A teetering system with free yaw is not prone to these problems (ref 2).

This leaves pitch/flap instabilities which are of concern. By studying the rotor mode shapes and noting pitch deflections are concentrated at the pitch axis a single blade analysis can be justified.

Out-of-plane vibration modes can be classified into two groups as either involving or not involving teeter. Figure 5 shows the first four out-of-plane mode shapes for a teetering rotor. The first and third (5a, 5c) involve a teetering motion with the flap deflections of each blade oppoOltte. Conversely, the second and third (5b, 5d) involve no teetering deflection and have identical flap deflections. Control pitch deflections, due to mechanical requirements of the pitch linkage, change the pitch angles of each blade by the same amount.

Pitch/flap instabilities involve an aerodynamic coupling of the above control pitch and out-of-plane deflections. The above then would require instabilities involving teeter motions to have a different mode shape for each blade. A 180 degree phase shift in pitch/flap deflections would have to occur. For this reason instabilities which involve a teetering motion are not anticipated. Other pitch/flap instabilities which involve cantilever deflections are however possible.

Note that pitch deflections due to a delta 3 angle, being directly coupled to teeter motions, are not independant degrees of freedom. This delta 3 effect will further stabilize modes which involve teeter motions (ref 3,4).

Three simple analytic models have been used to investigate pitch/flap aeroelasic stability. All involve rigid body, equivalent hinge representations. The first being a "classic" form derived from the helicopter industry. It incorporates Quasi-Steady, Theodorsen, aerodynamics with constant chord and twist (ref 5,6). The second uses the same formulation but assumes steady state aerodynamics. Figure 6 shows a representation of the first two models. The third model uses steady state aerodynamics but includes several geometric improvements over the first two. It includes twist and taper along with hinge offsets to better approximate geometric control characteristics. This model was derived for time domain investigations of control response. Figure 7 represents this model.

Each of these analytic models can be presented in matrix form as:

$$\frac{1}{\Omega^2}\begin{bmatrix} 1 & m_{\ddot\theta} \\ M_{\ddot\phi} & M_{\ddot\theta} \end{bmatrix}\begin{Bmatrix} \ddot\phi \\ \ddot\theta \end{Bmatrix} + \frac{1}{\Omega}\begin{bmatrix} m_{\dot\phi} & m_{\dot\theta} \\ M_{\dot\phi} & M_{\dot\theta} \end{bmatrix}\begin{Bmatrix} \dot\phi \\ \dot\theta \end{Bmatrix} + \begin{bmatrix} m_\phi & m_\theta \\ M_\phi & M_\theta \end{bmatrix}\begin{Bmatrix} \phi \\ \theta \end{Bmatrix}$$

$$= \begin{Bmatrix} m_v \\ M_v \end{Bmatrix} v + \begin{Bmatrix} m_o \\ M_o \end{Bmatrix}$$

The stability derivatives, here the matrix elements, are given in Table I for each of the theoretical models. A numerical eigen value approach was used to solve the unforced equations for stability information.

A pitch/flap instability was predicted in each case. An attempt has been made to understand the parameters involved with this instability and eliminate it. In doing so some understanding of the system and the models used has been gained.

Various parameters were changed to determine which have a significant effect on this instability. This resulted in three parameters being flap natural frequency, RPM, and pitch damping. RPM is determined by the static design and was kept as small as reasonable. This leaves flap natural frequency and pitch damping for adjustment. Figure 8 shows stability plots for each of the three analytical models. These are calculated for running RPM and show flap natural frequency versus pitch damping. The three agree in general, predicting the instability, but differ quantitatively.

The flap natural frequency can be adjusted but, without a change in blade sructure, this parameter can not be varied enough to stabilize the system. Since pitch deflections are concentrated at the pitch axis damping can be added. This solution was adopted although a damper, being mechanical, can fail and allow the system to become unstable. A vibration shut down is required. For reliability, dampers are placed at the pitch shaft to avoid linkage wear and fatigue. Although having a minimal impact, pitch damping will slow gust response.

Some insight can be gained about the three analytical models from the stability plots in Figure 8. Note that the first two models compare well with the only difference due to aerodynamics. The similarity of these plots may be misleading due to the very low torsional stiffness which tends to slow the motions and minimize the differences between steady and Quasi-steady aerodynamics. The steady state assumption is the more conservative. The third model is considerably less stable than the first two. The modeling differences between these are the control offsets, taper, twist, and sweep but it is not known how much effect each has.

### DYNAMIC RESPONSE

To assess dynamic control response the third model, with its forcing function, was solved in the time domain. A numerical solution was used to analytically model several wind gust cases.

Figure 9 shows pitch and flap response for a wind gust of 8 to 24 m/s in one second. This is felt to be an extreme gust which would be rarely encountered. The control system is responding within 1/4 second and the greatest out-of-plane load, corresponding to the greatest flap deflection, occurs at 1/2 second. This response is fast enough to relieve major blade loads. The largest out-of-plane load encountered is near one fourth the worst case load coming from high wind shut down conditions.

The rapid response is inherent with this control system. Translating blade loads into a control pitch involves only the pitch inertia.

Most control systems sense a condition, such as an RPM change, which involves a much larger inertia. Pitch damping, added for aeroelastic stability, does slow response time but is a minor effect. The plot presented in Figure 9 includes this damping.

## CONCLUSIONS

Analysis of the control system is complex but results in a relatively simple mechanical system with control response rapid enough to relieve gusts. This complexity is due to the interdependance of rotor geometry, system loads, dynamic response and aeroelastic stability.

The simple aeroelastic models used are not in close agreement. These simple models are important in SWECS design where large computer codes are usually not cost effective. Investigations to determine the critical parameters in these models, and compare results with test data, or the large computer codes (ref 7), would be useful.

## ACKNOWLEDGEMENT

## REFERENCES

1 Wilson,R.E., Lissaman,B.S., "Applied Aerodynamics of Wind Power Machines", Oregon State Univ., NTIS PB238594, July 1974.

2 Shue,D.T., "Effects of Tower Motion on the Dynamic Response of Windmill Rotors", MS Thesis, Dept. of Aero. & Astro., MIT, Feb. 1977.

3 Bramwell,ARS, "Helicopter Dynamics", Wiley & Sons, 1976.

4 Stoddard,F.S., "Structural Dynamics, Staility and Control of High Aspect Ratio Wind Turbines", Rockwell/DOE contract # PF 67025F, Dec. 1978.

5 Miller,R.H., Ellis,C.W., "Helicopter Blade Vibration & Flutter", Journal of the American Helicopter Soc., July 1956.

6 Loewy,R.G., "Review of Rotary Wing V/STOL Dynamic and Aeroelastic Problems", AIAA paper 69-202, Feb. 1969.

7 Spera,D.A., "Comparison of Computer Codes for Calculating Dynamic Loads in Wind Turbines", NASA-ERDA Structural Dynamics Workshop, Nov. 1977.

** "Development of a 4KW SWECS", North Wind Power Company, Rockwell/DOE contract #PF0B501C. (Forthcoming Design Reports for further information).

## NOMENCLATURE

a - lift curve slope
c - chord
$C_J$ - coef. of lift
$d_1$ - offset (Fig 2)
$d_t$ - offset (Fig 2)
$I$ - $I_q/I_b$
$I_q$ - flap moment of inertia
$I_r$ - pitch moment of inertia
$I_s$ - $I_q/I_b$
$I_R$ - cross product of inertia
m - blade mass
r - local radius
R - radius
$R_i$ - inner blade radius

$r_c$ - CG radius
V - gust wind velocity
$V_o$ - equilibrium wind velocity
$\phi$ - flap angle
$\gamma$ - lock number
$\theta$ - pitch angle deflection
$\theta_o$ - equilibrium pitch angle
$\rho$ - air density
$\chi_A$ - quarter chord/elas. axis
$\chi_1$ - quarter chord/CG offset
$\Omega$ - rotor angular velocity
$\omega_\phi$ - flap natural frequency
$\omega_\theta$ - pitch natural frequency
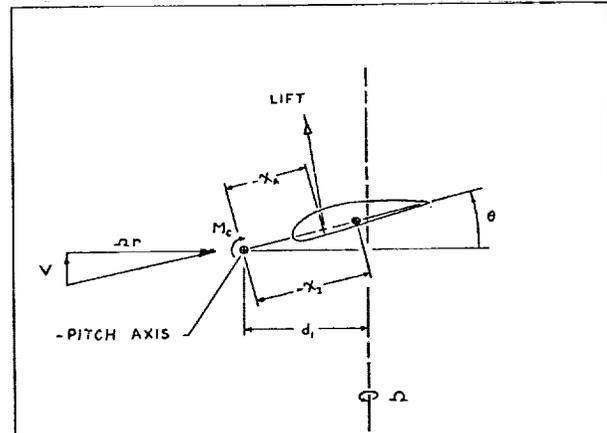


FIGURE 1 - CONTROL CONCEPT
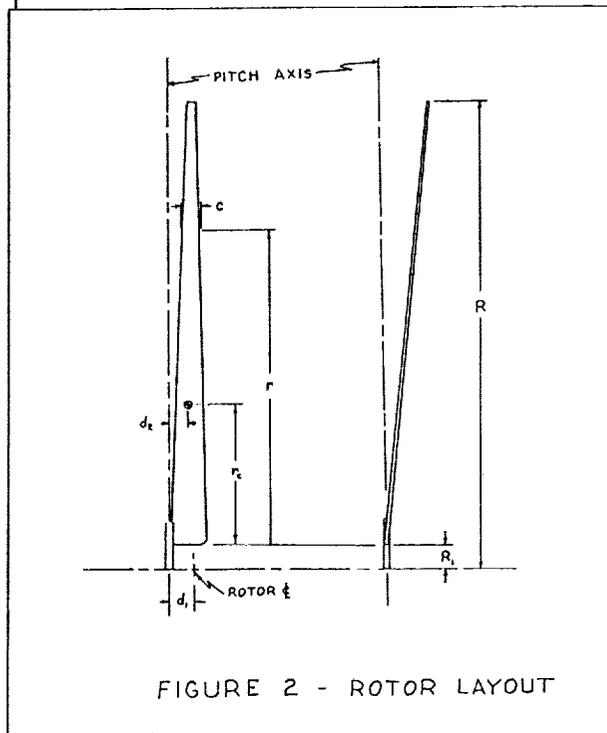


FIGURE 2 - ROTOR LAYOUT
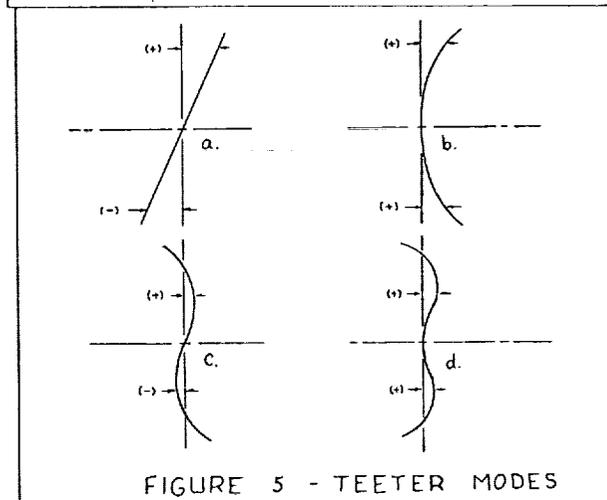


FIGURE 5 - TEETER MODES

FIGURE 4 - UNLOADED OVERSPEED

FIGURE 9 - GUST RESPONSE
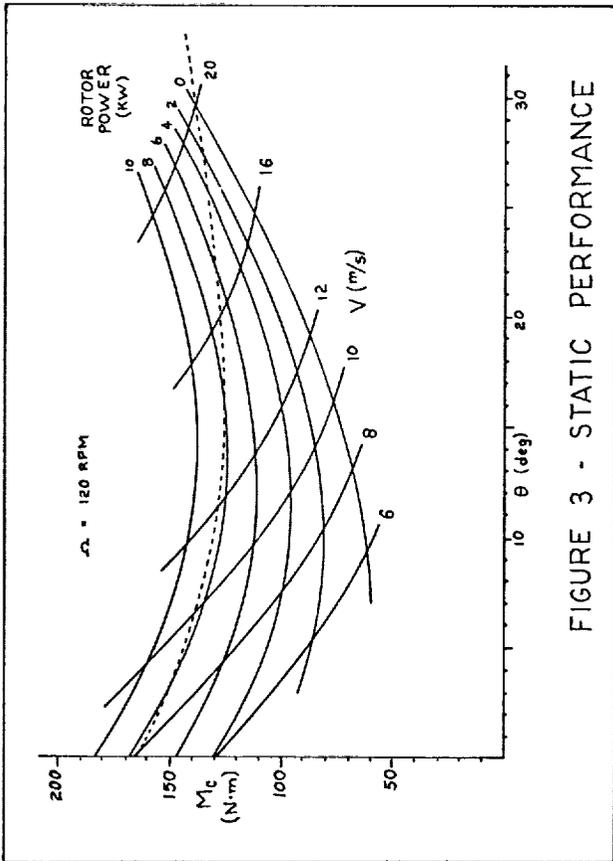
FIGURE 3 - STATIC PERFORMANCE

FIGURE 8 - STABILITY

UNIT VECTORS $a, b, e$ — MASS AXIS — ELASTIC AXIS — $\frac{c}{4}$ — $x_A$ — $x_I$ — $a_3, b_3$ — $e_3$ — $\beta$ — $b_2 e_2$ — $\theta$ — $a_2$ — ROTOR ℄ — $a_1$ — $e_1$ — $\theta$ — $\beta$ — $b_1$ — $\Omega$

FIGURE 6
MODELS 1 + 2



UNIT VECTOR. $a, b, e$ — MASS AXIS — ELASTIC AXIS — $\frac{c}{4}$ — $x_A$ — $x_I$ — $a_3, b_3$ — $e_3$ — $\theta$ — $d_2$ — $r_c$ — $b_2 e_2$ — $\theta$ — $a_2$ — PITCH AXIS — $a_1$ — $e_1$ — $\beta$ — $\theta$ — $b_1$ — $R_1$ — $d_1$ — ROTOR ℄ — $a_1$ — $\Omega$
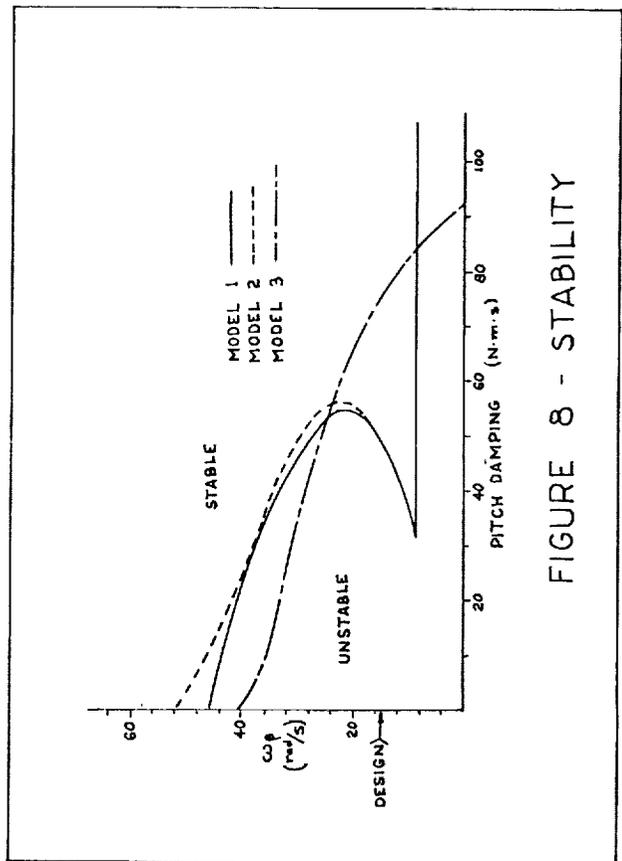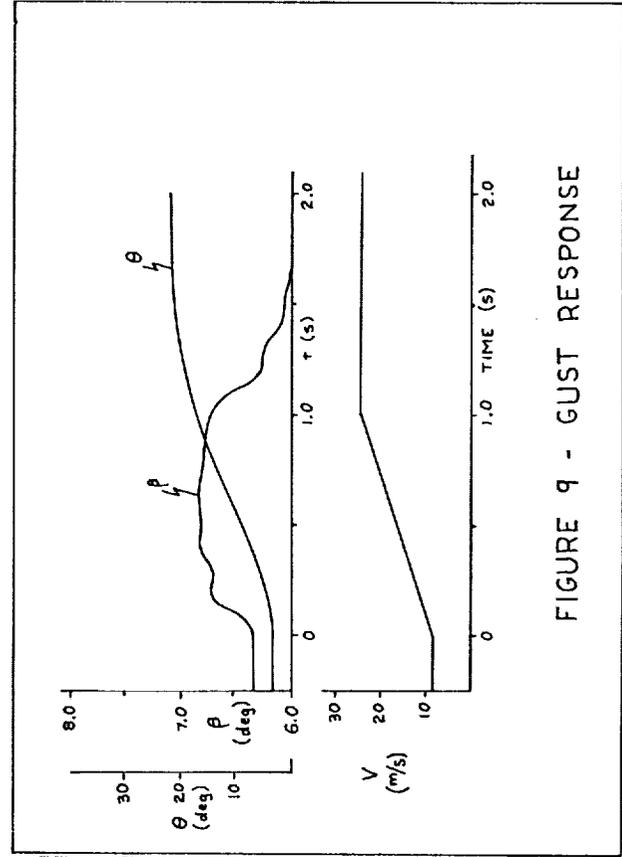
FIGURE 7
MODEL 3
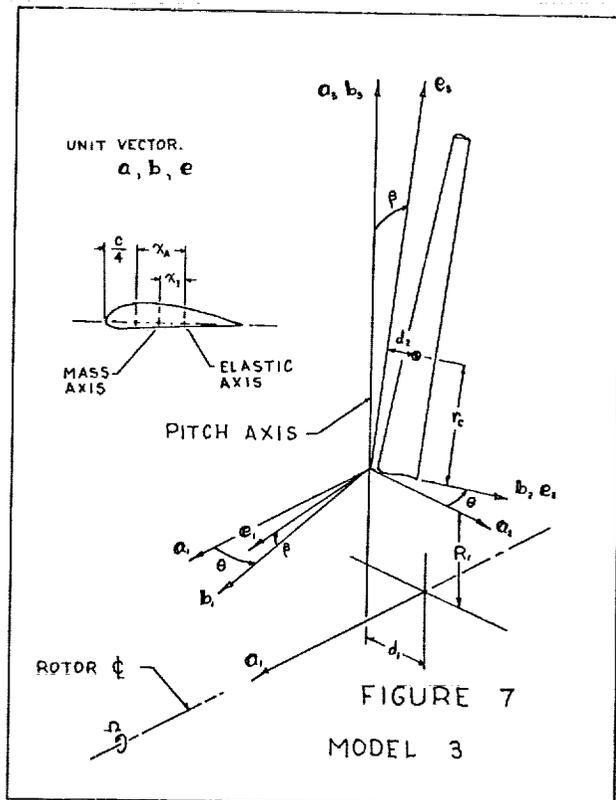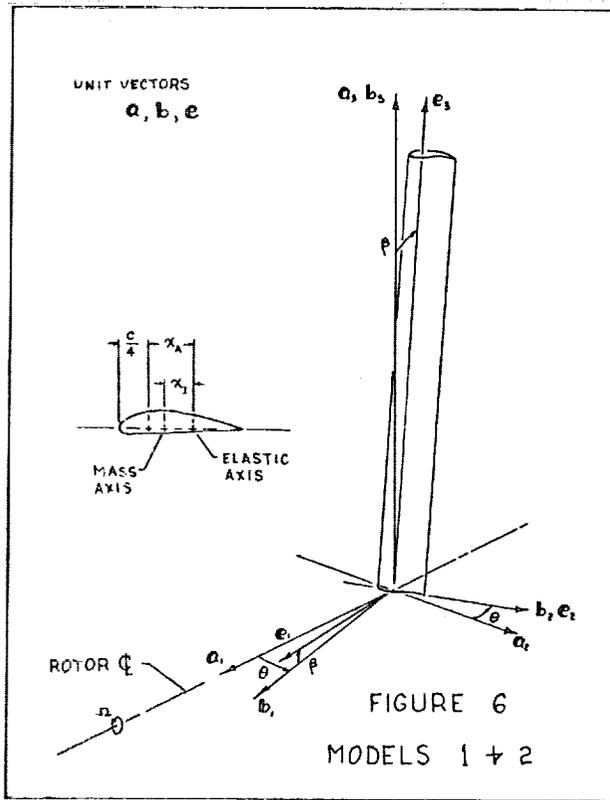
## TABLE I – STABILITY DERIVATIVES

| | MODEL 1 | MODEL 2 | MODEL 3 |
|---|---|---|---|
| $m_{\ddot\phi}$ | $\dfrac{\gamma}{8}$ | $\dfrac{\gamma}{8}$ | $\xi\displaystyle\int_0^{R-R_1} c\,r^2(R_1+r)(c\theta_o+\lambda s\theta_o)\,dr$ |
| $m_\phi$ | $1+\left(\dfrac{\omega_\phi}{\Omega}\right)^2$ | $1+\left(\dfrac{\omega_\phi}{\Omega}\right)^2+\dfrac{\gamma x_A}{6R}$ | $c^2\theta_o+\dfrac{mR_1 r_c}{I_b}+\left(\dfrac{\omega_\phi}{\Omega}\right)^2+\xi\displaystyle\int_0^{R-R_1} cr(R_1+r)(d_1+x_A c\theta_o)(c\theta_o+\lambda s\theta_o)\,dr$ |
| $m_{\ddot\psi}$ | $-I_x$ | $-I_x$ | $-I_x$ |
| $m_\psi$ | $\dfrac{\gamma}{6}\left[\dfrac{3c}{4R}-\dfrac{x_A}{R}\right]$ | $-\dfrac{\gamma x_A}{6R}$ | $-\xi\displaystyle\int_0^{R-R_1} cr(R_1+r)x_A(c\theta_o+\lambda s\theta_o)\,dr$ |
| $m_\theta$ | $-I_x+\dfrac{\gamma}{8}$ | $-I_x+\dfrac{\gamma}{8}$ | $-I_x c(2\theta_o)+\dfrac{mr_c d_1}{I_b}c\theta_o-\xi\displaystyle\int_0^{R-R_1} cr(R_1+r)^2\left[(\lambda^2-1)c(2\theta_o)-2\lambda s(2\theta_o)\right]dr$ |
| $M_{\ddot\psi}$ | $I$ | $I$ | $I$ |
| $M_\psi$ | $-\dfrac{\gamma}{2}\left[\dfrac{c}{8R}-\dfrac{x_A}{2R}\right]\left[\dfrac{x_A}{R}-\dfrac{c}{2R}\right]$ | $\dfrac{\gamma x_A^2}{4R^2}$ | $\xi\displaystyle\int_0^{R-R_1} c(R_1+r)x_A^2(c\theta_o+\lambda s\theta_o)\,dr$ |
| $M_\theta$ | $I\left[1+\left(\dfrac{\omega_\phi}{\Omega}\right)^2\right]-\dfrac{\gamma x_A}{6R}$ | $I\left[1+\left(\dfrac{\omega_\phi}{\Omega}\right)^2\right]-\dfrac{\gamma x_A}{6R}$ | $Ic(2\theta_o)-\dfrac{md_1 d_2}{I_b}c\theta_o+I\left(\dfrac{\omega_\phi}{\Omega}\right)^2-\xi\displaystyle\int_0^{R-R_1} c(R_1+r)^2 x_A\left[2\lambda s(2\theta_o)+(1-\lambda^2)c(2\theta_o)\right]dr$ |
| $M_{\ddot\phi}$ | $-I_x$ | $-I_x$ | $-I_x$ |
| $M_\phi$ | $-\dfrac{\gamma x_A}{6R}$ | $-\dfrac{\gamma x_A}{6R}$ | $-\xi\displaystyle\int_0^{R-R_1} cr(R_1+r)x_A(c\theta_o+\lambda s\theta_o)\,dr$ |
| $M_\phi$ | $-I_x$ | $-I_x-\dfrac{\gamma x_A^2}{4R^2}$ | $-I_x c(2\theta_o)-\dfrac{mr_c d_1}{I_b}c\theta_o$ $-\xi\displaystyle\int_0^{R-R_1} c(R_1+r)(c\theta_o+\lambda s\theta_o)\left[x_A(x_A c\theta_o+d_1)-\dfrac{c_d}{c_d+a}r(R_1+r)(c\theta_o+\lambda s\theta_o)\right]dr$ |

$$\gamma=\frac{\rho a R^4 c}{2 I_b}$$

$$m_o=-\tfrac{1}{2}I_x s(2\theta_o)-\frac{mr_c d_1}{I_b}s\theta_o+\xi\int_0^{R-R_1} cr(R_1+r)^2\left[\tfrac{1}{2}(\lambda^2-1)s(2\theta_o)+\lambda c(2\theta_o)-\frac{a}{c_d+a}\theta_r(c\theta_o+\lambda s\theta_o)^2\right]dr$$

$$M_o=-\tfrac{1}{2}I\,s(2\theta_o)+\frac{md_1 d_2}{I_b}s\theta_o-\xi\int_0^{R-R_1} cx_A(R_1+r)^2\left[\tfrac{1}{2}(\lambda^2-1)s(2\theta_o)+\lambda c(2\theta_o)-\frac{a}{c_d+a}\theta_r(c\theta_o+\lambda s\theta_o)^2\right]dr$$

$$m_v=\frac{\gamma}{\Omega}\int_0^{R-R_1} cr(R_1+r)\left[\lambda s(2\theta_o)+c(2\theta_o)\right]dr$$

$$M_v=-\frac{\gamma}{\Omega}\int_0^{R-R_1} cx_A(R_1+r)\left[\lambda s(2\theta_o)+c(2\theta_o)\right]dr$$

$$\xi=\frac{\rho(c_d+a)}{2 I_b}$$

$$\lambda=\frac{V_o}{\Omega(R_1+r)}$$

QUESTIONS AND ANSWERS

H. Currin

From:  T.A. Egolf

Q:  How does the nonlinearity of the actual unsteady lift response to rapid high angle
of attack variations affect the control system response?

A:  *Response should be rapid enough to avoid stall with any "real world" gust (an ad-
vantage of this control). Dynamic stall, if encountered, initially increasing lift
would increase pitch response. Wihtout stall, I'd guess unsteady aero would slow
response.*